Proc. Natl. Acad. Sci. USA
Vol. 83, pp. 3547–3551, May 1986
Physiological Sciences

Fusion of renal epithelial cells: A model for studying cellular mechanisms of ion transport

(diluting segment/furosemide/amiloride/cell membrane potential)

H. OBERLEITHNER, B. SCHMIDT, AND P. DIETL

University of Würzburg, Medical School, Department of Physiology, Röntgenring 9, 8700 Würzburg, Federal Republic of Germany

Communicated by Gerhard Giebisch, December 27, 1985

ABSTRACT **The investigation of epithelial ion transport at the cellular level by means of electrophysiological techniques is hampered by the small size of epithelial cells. Moreover, interpretation of experiments is complex due to poorly defined and highly variable paracellular leaks (shunt pathways). In search of a new experimental approach we developed a technique to isolate renal epithelial cells (diameter ≈ 10 μm) from diluting segments of the frog kidney and to fuse them to "*giant*" cells (diameter ≈ 100 μm). These cells generate membrane potentials of −54.1 ± 1.6 mV (mean ± SEM; n = 40). They are sensitive to the diuretic drugs furosemide and amiloride and to the K^+- and Cl^--permeability blockers Ba^{2+} and anthracene-9-carboxylic acid. The experiments demonstrate membrane potential measurements in cells isolated from renal epithelium and fused to giant cells. The cells retain their specific membrane properties and could serve as a valuable experimental model in epithelial research.**

The kidney is known as a target organ for various peptide and steroid hormones. To trace hormone-induced intracellular events in the living epithelial cell, conventional and ion-sensitive microelectrodes can be inserted into the cell cytosol for continuous measurement of cell membrane potentials and ion activities. This could be done most adequately in a single cell preparation in well-defined extracellular medium. We planned to perform the experiments in cells of the diluting segment of the frog kidney because basic transport mechanisms are sufficiently described in this epithelium (1, 2) and because amphibian kidneys are handled more easily compared to the mammalian preparation. In contrast to our own expectations, it appeared impossible to perform reliable intracellular measurements in a single epithelial cell due to irreversible cell damage during impalement. We thought that a significant magnification of the cell size could possibly overcome this problem. Therefore, we fused single renal cells to "*giant*" epithelial cells. The paper describes the fusion procedure, the gross morphology, and the basic functional properties of these giant cells.

METHODS

We describe the procedure of (*i*) isolating cells of a distinct nephron segment (i.e., the diluting segment), (*ii*) fusing the single cells to giant cells, and (*iii*) performing intracellular potential measurements while viewing the cell under study with high-resolution differential interference-contrast microscopy (Fig. 1).

Kidneys of *Rana pipiens* were perfused according to techniques published in detail (3). For the preparation of frog renal cells we modified the two-step method reported for the isolation of liver cells (4, 5): to break up the intercellular junctions, both kidneys were perfused via the aorta with Ca^{2+}/Mg^{2+}-free amphibian Ringer solution (50 ml, 10 min) composed of (mM) 97 NaCl, 3 KCl, and 10 Hepes titrated to pH of 7.8 by 0.1 M NaOH. In a second step, the kidneys were perfused (10 ml, 2 min) via the portal veins with amphibian Ringer solution containing Ca^{2+} (1.5 mM), Mg^{2+} (1.0 mM), and collagenase (0.05%, 180 units/mg; Sigma, Munich, F.R.G.) to dissolve the intercellular matrix. By means of fine scissors superficial portions of 2–3 mm^2 (thickness, 1 mm) were removed from the ventral surface of the kidney. These kidney fragments contain almost exclusively *diluting* segments.

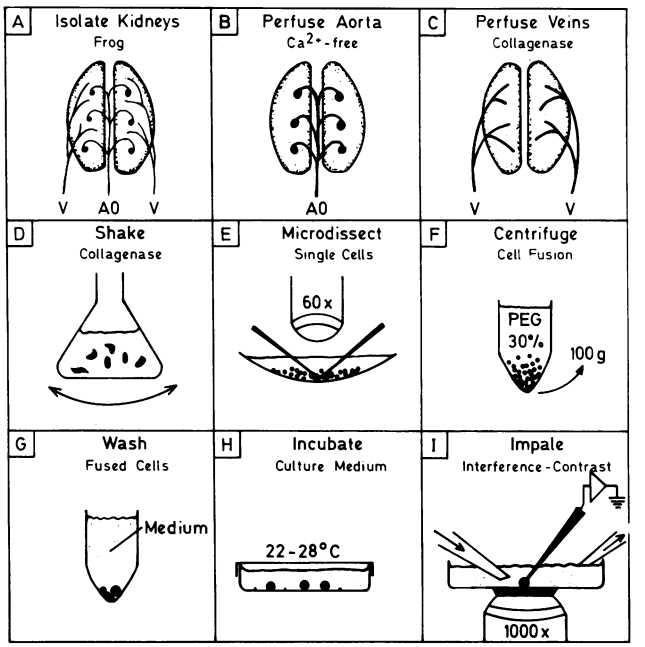

FIG. 1. Single steps from kidney isolation via cell fusion to the successful intracellular impalement.

The fragments were transferred to a glass vial with 10 ml of the collagenase-containing kidney perfusate and were shaken gently for 10 min at standardized temperature (28°C). Then, the kidney fragments were microdissected by needles in the presence of 100 μl of the collagenase-containing solution. Thus, the epithelial structure was dissolved and the individual tubule cells could be collected by a Pasteur pipette. They were transferred into a conical tube containing the fusion medium. This consisted of 30% polyethylene glycol (PEG, M_r 4000) dissolved in Leibovitz-15 medium. The fusion medium was diluted to 275 mosM/liter, buffered with 10 mM Hepes, and titrated to an apparent pH of 8.6. Since pH measurements in the fusion medium by means of pH-sensitive glass electrodes turned out to be unreliable (probably due to interaction of PEG with the glass electrode), phenol red was added and the fusion medium was titrated with 0.1 M NaOH until the indicator had changed completely from yellow to red. After centrifugation (100 × *g*, 3 min) the

The publication costs of this article were defrayed in part by page charge payment. This article must therefore be hereby marked "*advertisement*" in accordance with 18 U.S.C. §1734 solely to indicate this fact.

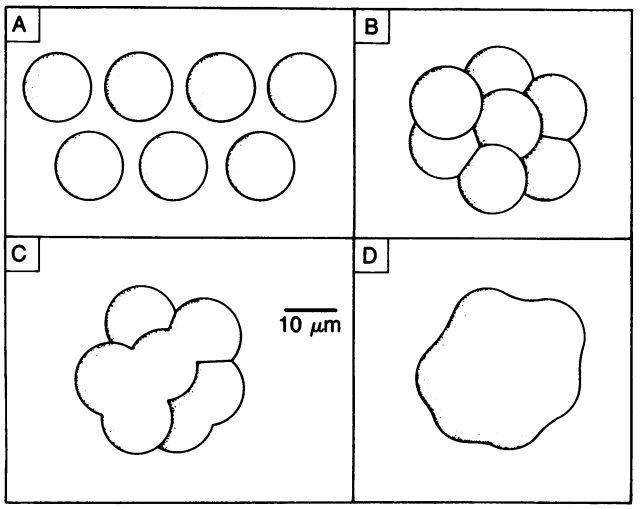

FIG. 2. Single steps of renal epithelial cell fusion. (*A*) Before fusion. (*B*) During fusion. (*C*) Ten minutes after fusion. (*D*) Two hundred forty minutes after fusion.

supernatant was removed and the cell pellet was washed in modified serum-free Leibovitz-15 medium (diluted to 200 mosM/liter; 100 mg of penicillin/streptomycin per liter). The mixture, containing single cells and fused cells, was finally transferred onto a thin microscope coverslip that was pre-treated with poly(lysine) [poly(L-lysine), 1 g/liter; Serva, Heidelberg, F.R.G.]. A polyvinyl chloride ring (diameter, 25 mm; 1 mm in height) had been glued on the coverslip. Thus, more culture medium could be added (≈1 ml) and the cells were incubated for the next 4 hr at a temperature between 22°C and 28°C.

Out of about 10^4 early-distal tubule cells that could be harvested from the two kidneys, some 5–10 giant cells could be formed. Each giant cell was composed of ≈50–200 single cells; the rest remained unfused. Healthy giant cells and single cells were found attached to the bottom of the coverslip within 60 s. Applying high-resolution differential-contrast microscopy, the outlines of the single cells could be still detected within a giant cell a few minutes after the PEG-fusion step but disappeared within the following hours (Fig. 2). After about 4 hr, the giant epithelial cells had reached their final shapes. They were found well attached to the glass surface, were homogeneous in structure, and did not accumulate trypan blue.

After the 4-hr incubation period, superfusion was started with amphibian Ringer solution that could be rapidly changed to various test solutions while cell membrane potential measurements were performed applying standard electrophysiological techniques. Cell impalements were performed with microelectrodes (filled with 0.1 M KCl; input resistance, 400–600 MΩ) while giant cells under study could be observed by means of an inverted microscope (Zeiss IM 35, differential interference-contrast, objective lens 100/1.25, oil).

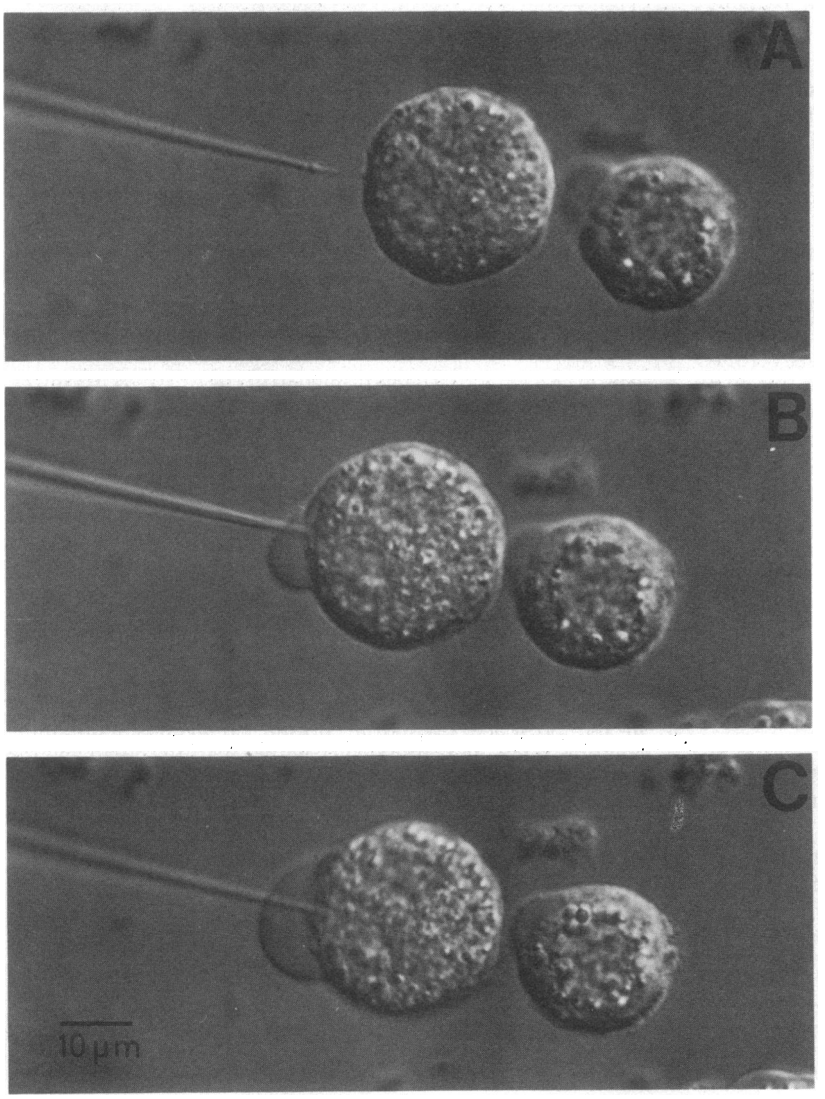

FIG. 3. Intracellular potential measurement in a single cell of the diluting segment of frog kidney. The cell was superfused with amphibian control solution. (*A*) The tip of a microelectrode (filled with 0.1 M KCl; input resistance, 400 MΩ) was moved close to the cell membrane. (*B*) The cell was impaled by advancing the microelectrode stepwise (0.5-μm steps) using a piezoelectric device. A cell membrane potential of −25 mV was measured, which collapsed within 10 s to −5 mV; simultaneously cell swelling occurred. (*C*) Thirty seconds after impalement. The cell membrane potential had dissipated completely. Cell swelling had reached its maximum and was found to be irreversible. A few seconds later, the cell got loose and was washed off by the superfusate.

The results are given as single or mean values, ± SEM.

RESULTS

Fig. 3 illustrates the morphological changes of a single renal cell of frog diluting segment induced by the intracellular impalement. The observed cell swelling starts a few seconds after insertion of the microelectrode tip into the cell cytosol. The cell remains damaged even when the microelectrode tip is withdrawn from the cell interior. The cell impalement is accompanied by an immediate negative shift of the microelectrode reading of some 10–30 mV (cell interior negative vs. bath-ground) followed by a rapid decline of the cell membrane potential to a value near zero. The decay of the cell membrane potential after the impalement correlates temporally tight with the observed cell swelling.

Intracellular measurements in fused cells (Fig. 4) with diameters of ≥50 μm are markedly different. No cell swelling occurs after insertion of the microelectrode tip into the cell interior. Cell impalements remain stable for hours. The electrode can be withdrawn and reinserted several times in the same cell without a significant decay of the membrane potential. Directly after the fusion process, cell borders of single cells can be detected within the giant cell by means of high-resolution interference-contrast microscopy. Within hours following the fusion step, individual cell borders become less detectable and the giant cell approaches a spherical shape (compare Fig. 2). Intracellular impalements immediately after the fusion process were usually not successful. This is probably due to the fact that initially (i.e., during PEG exposure) cell clusters were formed composed of tightly packed single cells. As illustrated in Fig. 2, the cell fusion process lasts for hours. It seems completed after about 4 hr. Then, no cell borders are visible within the giant cell and cell membrane potential measurements are stable.

Fig. 5 *Upper* illustrates that at least 15 single cells must fuse to one giant cell, which then allows reliable intracellular impalements. A further increase of the cell size does not influence the absolute magnitude of the membrane potential. The frequency distribution of the cell membrane potentials of 40 fused cells with diameters of ≥50 μm is shown in Fig. 5 *Lower*. The mean value of V_m is −54.1 ± 1.6 mV. All impalements included in Fig. 5 were performed at least 4 hr after exposure to PEG. The cells were homogeneous in structure and virtually spherical in shape.

To test whether the giant cell retains the cell membrane properties of the individual epithelial cell, transport inhibitors were applied and ion concentration changes were performed in the bath medium. The data are summarized in Fig. 6. Furosemide and anthracene-9-carboxylic acid both hyperpolarize V_m. This is in full agreement with previous observations in the intact epithelium (1, 6). The cell membrane has significant K^+ and Cl^- conductances, which are detected by the K^+- and Cl^--induced V_m changes. Ba^{2+} blocks the K^+ channels of the cell and thus depolarizes V_m and eliminates

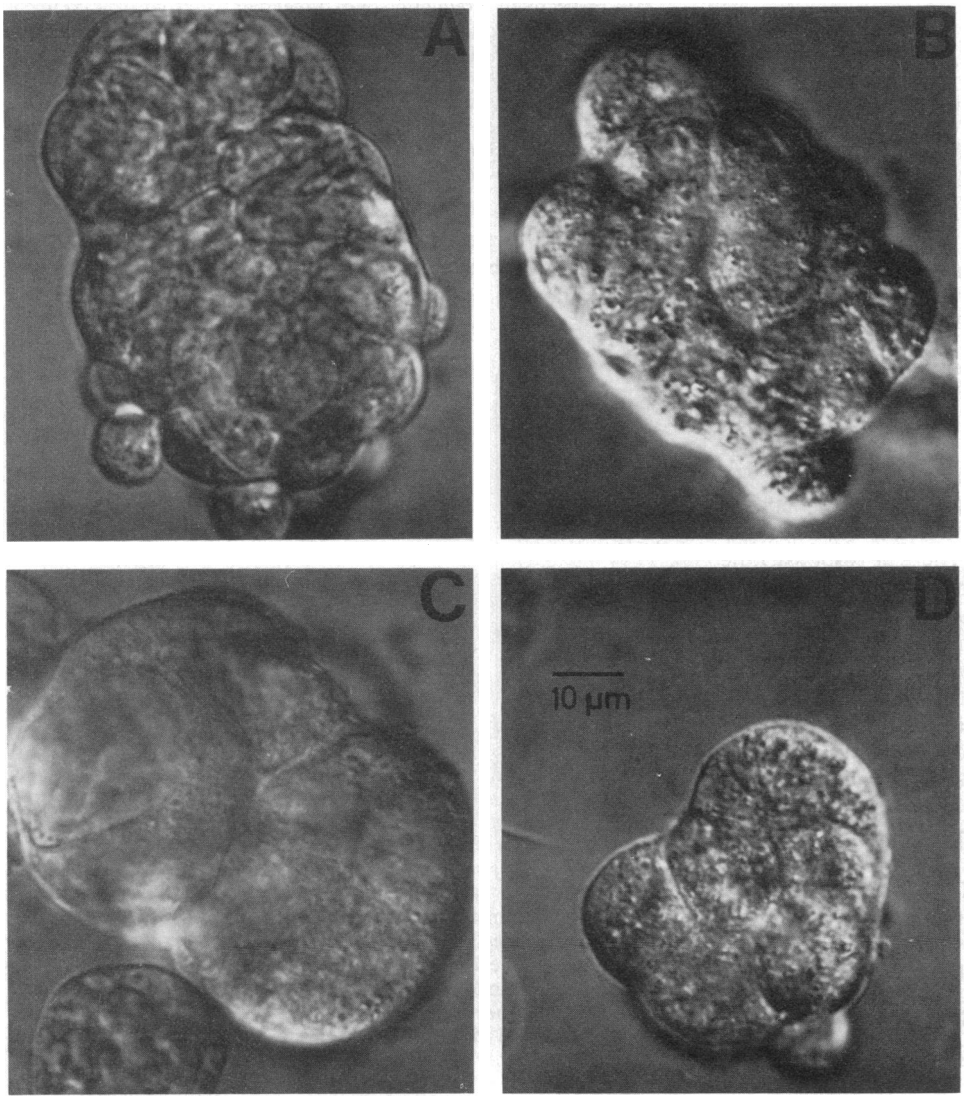

FIG. 4. Giant renal epithelial cells obtained after fusion of single cells from frog diluting segment. The cells were incubated in modified Leibovitz-15 medium for 4 hr before intracellular measurements were started. The individual cell membrane potentials remained stable for at least 30 min and were −56, −62, −58, and −50 mV in *A*, *B*, *C*, and *D*, respectively. All photographs were taken after the impalements; no cell swelling occurred, even after several impalements of one individual giant cell.

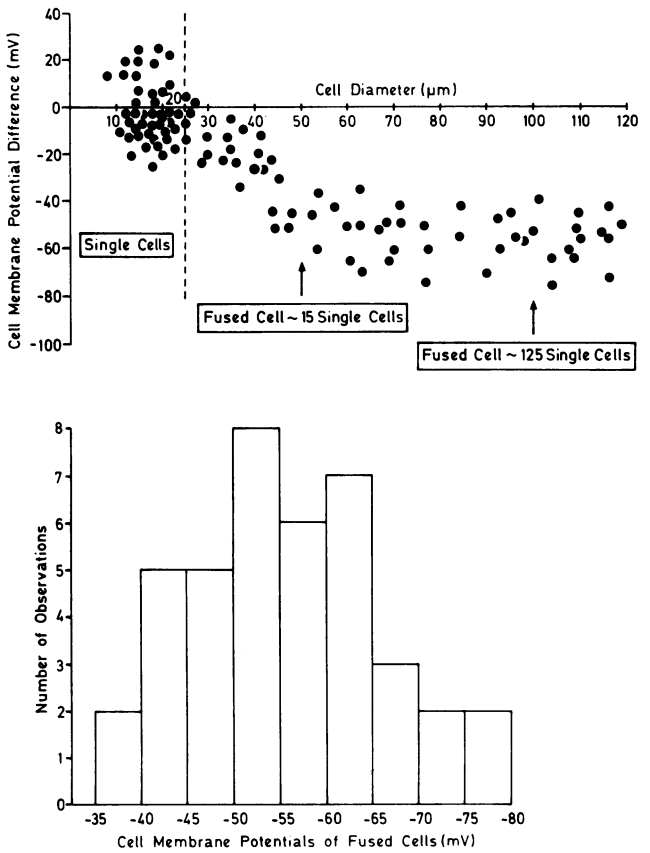

FIG. 5. (*Upper*) Cell membrane potentials of early-distal tubule cells were plotted as a function of cell diameter. The potential measurements were performed in single and fused cells of various sizes at least 4 hr after isolation. Microelectrodes were filled with 0.1 M KCl and had input resistances of 400–600 MΩ. Cell membrane potentials remained stable only in fused cells with cell diameters of ≥50 μm. Impalements of single cells and of small fused cells were leaky, cell membrane potentials dissipated within seconds to a few minutes, and simultaneously cell swelling occurred (see Fig. 3). Since most fused cells were approximately spherical, we estimated the number of single cells fused to one giant cell from the respective radii of single and fused cells. (*Lower*) Frequency distribution of cell membrane potentials of fused cells (≥50 μm) from early-distal tubule of frog kidney. The mean value for 40 fused cells was −54.1 ± 1.6 mV.

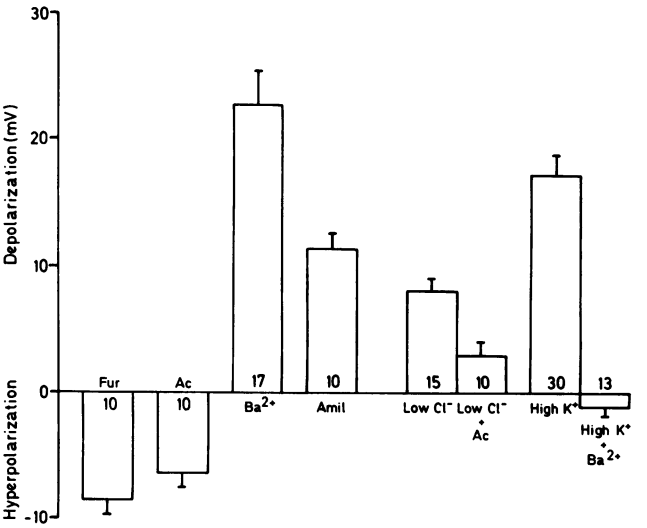

FIG. 6. Effect of ion transport inhibitors, of permeability blockers, and of Cl^- and K^+ concentration step changes on cell membrane potentials in fused cells of early-distal tubule. The $Na^+/K^+/Cl^-$ cotransport inhibitor furosemide (Fur, 0.05 mM) and the Cl^- permeability blocker anthracene-9-carboxylic acid (Ac, 0.1 mM) hyperpolarized the cell membrane for 8.5 ± 0.9 mV and 6.4 ± 0.9 mV, respectively. The K^+ permeability blocker barium (Ba^{2+}, 3 mM) and the Na^+/H^+ exchange inhibitor amiloride (Amil, 1 mM) depolarized the cell membrane potentials for 22.8 ± 2.6 mV and 11.5 ± 1.1 mV, respectively. Reduction of extracellular Cl^- from 105 mM to 55 mM (low Cl^-, Cl^- substituted by gluconate) led to a transient depolarization of the cell membrane of 8.2 ± 0.7 mV. This transient decrease of V_m was found significantly ($P < 0.01$) reduced to 3.1 ± 0.9 mV in the presence of Ac (0.1 mM). The increase of extracellular K^+ (K^+ substituted for Na^+) depolarized V_m for 17.4 ± 1.5 mV. This effect could be completely inhibited by Ba^{2+} (3 mM). The number within each bar = the number of observations.

the K^+-induced change of V_m. Amiloride inhibits Na^+/H^+ exchange, as known from the intact epithelium, and depolarizes V_m, probably via intracellular acidification and secondary inhibition of K^+ conductance (7). The 95% response time of the various drug-induced V_m changes ranged between 5 and 20 s; all effects were fully reversible.

Fig. 7 gives a further insight into the mechanism of action of furosemide. On the other hand, hyperpolarization of V_m, induced by the diuretic, is marked at low extracellular K^+. On the other hand, the furosemide-induced voltage change approaches zero when K^+ is elevated to 15 mM in the bath medium. The fact that decreasing bath K^+ concentration to low values leads to a nonlinear relationship between V_m and extracellular K^+ indicates the presence of another conductive ionic pathway, most likely one for chloride. This is strongly supported by the observation that with passive distribution of Cl^- across the cell membrane—namely, after addition of furosemide—V_m shifts to values expected to be close to the transmembrane K^+ equilibrium potential.

DISCUSSION

Although application of electrophysiological techniques in intact epithelia greatly enhanced our knowledge on the underlying mechanisms of transepithelial ion transport (8), it appears desirable to investigate individual membrane properties, active (i.e., ion pumps) and passive (i.e., ion perme-

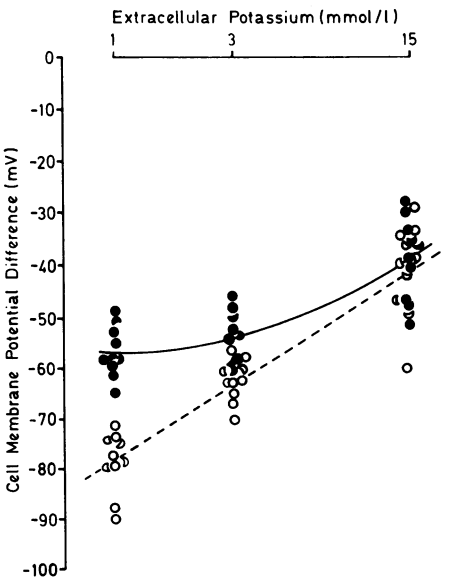

FIG. 7. Cell membrane potentials of fused cells are plotted as a function of extracellular K^+ concentration. Paired experiments were performed in the absence (closed symbols) and presence (open symbols) of 0.05 mM furosemide in the bath medium. In the absence of furosemide, the mean value of V_m at extracellular K^+ concentrations of 1, 3, and 15 mM was −57.1 ± 1.5, −54.6 ± 1.8, and −38.6 ± 2.5 mV, respectively. In the presence of furosemide, V_m averaged −78.9 ± 1.8, −63.1 ± 1.3, and −41.9 ± 2.8 mV, respectively.

abilities) transport processes, hormone-induced intracellular events, etc., in the isolated epithelial cell. Then, cell-to-cell (9) and paracellular (10) shunt pathways cannot interact and limit the interpretation of the experiments.

However, we were not able to get stable intracellular impalements of single renal cells. A few seconds after impalement, irreversible cell swelling occurred (Fig. 1) and V_m dissipated. Varying electrode filling solutions according to previous reports (11), using high-resistance (400–600 MΩ) microelectrodes with ultrafine tips, and applying piezoelectric devices for cell impalements with adequate optical control (interference-contrast) could not improve the yield of acceptable intracellular recordings. Since intracellular impalements can be performed successfully in the intact renal epithelium (1, 2, 7), the question arises why this cannot be achieved when the cell is removed from its physiological environment. Epithelial cells are usually coupled via intercellular (gap) junctions (9). These allow current flow between cells. We assume that current flow between cells compensates for transient impalement damage. Thus, the intracellular potential of an impaled cell in an intact epithelium is maintained by the electromotive forces of the neighboring cells. Impaling a single epithelial cell, isolated from neighboring cells, leads to an irreversible depolarization of the cell membrane. We assume that in depolarized cells of frog diluting segment, Cl^- ions enter the cell interior via the Cl^--permeable (6) cell membrane, driven by a favorable electrochemical gradient. As a result, the cell swells irreversibly.

Fusion of single renal epithelial cells to giant cells eliminates this problem. Intracellular impalements of cells with diameters beyond 50 μm are stable for hours. If the giant cells are incubated at room temperature (or at 4°C) in modified Leibovitz-15 medium, they can be studied up to at least 20 hr after fusion. We assume that the crucial improvement was the dramatic increase of the volume over surface ratio of the cell.

Fusion of animal cells has become an important tool in experimental cell research (12, 13). Successful application of the PEG method for cell fusion requires careful evaluation of the most important parameters (14) and adequate adjustment to the individual biological preparation. We tested PEG of different molecular weights at different concentrations; we varied the temperature and the length of the fusion step and the pH and the Ca^{2+} concentration in the fusion medium; we also tested kidneys of several animal species (*Rana pipiens, Rana catesbejana, Xenopus laevis, Amphiuma*). So far, the above described method gives the best yield on intact fused cells. A totally different fusion technique, electric field-induced fusion, could be also a promising approach (15).

It is a striking observation that the cell fusion procedure obviously does not affect qualitatively the specific cell membrane properties of the early-distal cells. Transport inhibitors (furosemide, amiloride) and permeability blockers (Ba^{2+}, anthracene-9-carboxylic acid) exert effects on V_m that compare well with the action of these substances in the intact epithelium (1, 2, 6). Moreover, the characteristic functional responsiveness indicates that the fused giant cell is indeed composed of cells of the diluting segment. Furosemide and anthracene-9-carboxylic acid hyperpolarize V_m by two different mechanisms: whereas furosemide inhibits the inwardly directed $Na^+/K^+/Cl^-$ cotransport system (1, 2), anthracene-9-carboxylic acid inhibits Cl^- exit from the cell cytosol by reducing Cl^- conductance (6, 16, 17). The existence of a significant Cl^- conductance and its inhibition by anthracene-9-carboxylic acid is confirmed by the V_m changes induced by Cl^- concentration steps. Either inhibition of intracellular Cl^- accumulation by furosemide or elimination of a significant Cl^- conductance will drive V_m close to the transmembrane K^+ equilibrium potential (18). The large K^+-induced depolarization indicates a significant K^+ conductance of the cell membrane that can be inhibited completely by Ba^{2+} ions. From the Cl^-- and K^+-induced V_m changes, the transference numbers of these specific ions can be estimated; they are approximately 0.6 and 0.4, respectively. This indicates that in the presence of Hepes-buffered (i.e., HCO_3^-/CO_2 free) extracellular medium, the Cl^- and K^+ conductances represent the major conductive pathways of the cell membrane. Amiloride inhibits Na^+/H^+ exchange in this epithelium (7). Amiloride-induced depolarization of V_m is most likely caused by a decrease of the K^+ conductance in response to intracellular acidosis (7). Fig. 7 demonstrates the dependence of V_m on extracellular K^+. With decreasing extracellular K^+, the K^+ conductance of the cell membrane vanishes and V_m approaches the transmembrane Cl^- equilibrium potential (1, 6). The situation changes dramatically when the Cl^--uptake mechanism is inhibited by furosemide. Then, Cl^- ions will be passively distributed across the cell membrane and V_m will switch back to values close to the K^+ equilibrium potential (18). These observations support experimental data from intact epithelium of the amphibian (1, 2) and the comparable mammalian (19) preparation.

Although the transport properties of the cell membranes of the giant cells are qualitatively similar to the native single cells that originally formed the diluting segment, we must assume that the polarity of the epithelial cell has disappeared. The electromotive forces of the individual cell membranes are now short-circuited. Most likely, ion channels and ion pumps are distributed randomly throughout the cell membrane. Furthermore, we cannot rule out the possibility that ion channels of one kind form clusters in one part, while other channels accumulate in other parts of the cell surface, thus giving rise to undefined local current loops.

Nevertheless, the present experiments indicate that the fused epithelial cell could serve as a suitable model to study the cellular mechanisms involved in the origin, maintenance, and regulation of the cell membrane potential.

We thank Dr. S. Silbernagl and Dr. W. Wang for stimulating discussions, Mrs. M. Schulze for phototechnical assistance, and Mrs. I. Ramoz and I. Schönberger for typing the manuscript. The diuretics furosemide and amiloride were kindly provided by Hoechst Co., Frankfurt/Main, and by Frosst Pharma GmbH, Munich, F.R.G. This project is supported by Deutsche Forschungsgemeinschaft (SFB-176, A-6).

1. Oberleithner, H., Guggino, W. & Giebisch, G. (1982) *Am. J. Physiol.* **42,** F331–F339.
2. Guggino, W. B., Oberleithner, H. & Giebisch, G. (1985) *J. Gen. Physiol.* **86,** 31–58.
3. Oberleithner, H., Lang, F., Messner, G. & Wang, W. (1984) *Pflügers Arch.* **402,** 272–280.
4. Seglen, P. O. (1973) *Exp. Cell Res.* **76,** 25–30.
5. Graf, J., Gautam, A. & Boyer, J. L. (1984) *Proc. Natl. Acad. Sci. USA* **81,** 6516–6520.
6. Oberleithner, H., Ritter, M., Lang, F. & Guggino, W. (1983) *Pflügers Arch.* **398,** 172–174.
7. Oberleithner, H. (1985) *Pflügers Arch.* **404,** 244–251.
8. Diamond, J. M. (1982) *Nature (London)* **300,** 683–685.
9. Kanno, Y. & Loewenstein, W. R. (1966) *Nature (London)* **212,** 629–630.
10. Boulpaep, E. L. & Sackin, H. (1980) *Curr. Top. Membr. Transp.* **13,** 169–197.
11. Blatt, M. R. & Slayman, C. L. (1983) *J. Membr. Biol.* **72,** 223–234.
12. Köhler, G. & Milstein, C. (1975) *Nature (London)* **256,** 495–497.
13. Galfre, G., Howe, S. C. & Milstein, C. (1977) *Nature (London)* **266,** 550–552.
14. Westerwoudt, R. J. (1985) *J. Immunol. Methods* **77,** 181–196.
15. Zimmermann, U. & Vienken, J. (1982) *J. Membr. Biol.* **67,** 165–182.
16. Bryant, S. H. & Morales-Aquilera, A. (1971) *Am. J. Physiol.* **219,** 367–383.
17. Palade, P. T. & Barchi, R. L. (1977) *J. Gen. Physiol.* **69,** 879–896.
18. Oberleithner, H., Guggino, W. & Giebisch, G. (1983) *Pflügers Arch.* **396,** 185–191.
19. Greger, R. (1985) *Physiol. Rev.* **65,** 761–797.